Brillouin-Kerr Soliton Frequency Combs in an Optical Microresonator

Yan Bai,[1,*] Menghua Zhang,[1,*] Qi Shi,[1,*] Shulin Ding,[1,*] Yingchun Qin,[1] Zhenda Xie,[1] Xiaoshun Jiang,[1,†] and Min Xiao[1,2]

[1]National Laboratory of Solid State Microstructures, College of Engineering and Applied Sciences, and School of Physics, Nanjing University, Nanjing 210093, China

[2]Department of Physics, University of Arkansas, Fayetteville, Arkansas 72701, USA

(Received 26 June 2020; accepted 21 December 2020; published 10 February 2021)

By generating a Brillouin laser in an optical microresonator, we realize a soliton Kerr microcomb through exciting the Kerr frequency comb using the generated Brillouin laser in the same cavity. The intracavity Brillouin laser pumping scheme enables us to access the soliton states with a blue-detuned input pump. Because of the ultranarrow linewidth and the low-noise properties of the generated Brillouin laser, the observed soliton microcomb exhibits narrow-linewidth comb lines and stable repetition rate. Also, we demonstrate a low-noise microwave signal with phase noise of −49 dBc/Hz at 10 Hz, −130 dBc/Hz at 10 kHz, and −149 dBc/Hz at 1 MHz offsets for a 10.43 GHz carrier with only a free-running input pump. The easy operation of the Brillouin-Kerr soliton microcomb with excellent performance makes our scheme promising for practical applications.

DOI: 10.1103/PhysRevLett.126.063901

Owing to the advantages of the soliton frequency comb [1,2] in microresonators such as broad spectrum span, high repetition rate as well as on-chip integration, the soliton microcombs have been widely used in coherent optical communications [3], low-noise microwave signal generation [4–6], dual-comb spectroscopy [7,8], ultrafast optical ranging [9,10], astronomical spectrometer calibration [11,12], optical coherence tomography [13], optical frequency synthesizer [14], and optical atomic clock [15]. Although the soliton microcombs have many promises and have been achieved in several material platforms [1,2,16], they usually need special techniques to stably approach the soliton states due to the large thermo-optic nonlinearity in high-Q microcavity and red-pump-detuning requirement [17] for soliton generation. Also, despite the fact that soliton generation has been stably accessed in Si_3N_4 microresonators that have extremely low thermal absorption [18] by just using a slow laser tuning method [19], complicated deposition and thermal annealing procedures are normally required to achieve such low thermal absorption loss in Si_3N_4. So far, a number of schemes including power kicking [20,21], fast thermal tuning [22], pulsed laser driving [23], single sideband modulation [24], and using an auxiliary laser [25–27] have been used to fast tune the laser frequency or compensate the thermo-optic effect in high-Q optical microresonators. However, most of those methods require additional optical and electrical components, which make the soliton generation complicated and difficult for full on-chip integration.

In addition to the parametric nonlinearity that is used for Kerr soliton microcomb generation [1,2], stimulated Brillouin scattering (SBS) [28] is another interesting nonlinear optical effect in high-Q optical microresonators. In previous work, due to the high gain and narrow band of the SBS process, the SBS effect in microcavity has been used for producing on-chip ultranarrow linewidth laser [29,30], which further leads to the applications in Brillouin gyroscope [31] and low-noise microwave signal generation [32]. Despite the fact that the simultaneous presence of Brillouin laser and parametric oscillation were demonstrated in fiber Fabry-Perot (FP) cavity [33], microbottle [34], as well as microbubble cavities [35], yet no soliton microcomb with Brillouin lasing has been observed so far. Very recently, multisoliton Kerr comb was realized in a large size fiber cavity with intracavity multiple-wavelength Brillouin lasers [36]. However, no detail theoretical analysis was provided and the single-soliton operation was not observed.

In this Letter, we report a new approach for efficient generation of the soliton microcomb in a high-Q microresonator by producing a narrow-linewidth Brillouin laser first and then using this intracavity Brillouin laser to generate the Kerr frequency comb in the same cavity [Fig. 1(a)]. By properly selecting the mode spacing between the pump and Brillouin modes in combination with the Kerr self-phase modulation, we can achieve a red-detuned Brillouin laser with a blue-detuned input pump, which results in long soliton steps and enables stable access to the single soliton state by simply tuning the laser piezo. In addition, this approach is capable of self-stabilizing the system because of the thermo-optic nonlinearity [37]. This new type of soliton Kerr microcomb features narrow-linewidth comb lines and stable repetition rate. Besides, in this work we have further realized a low-noise

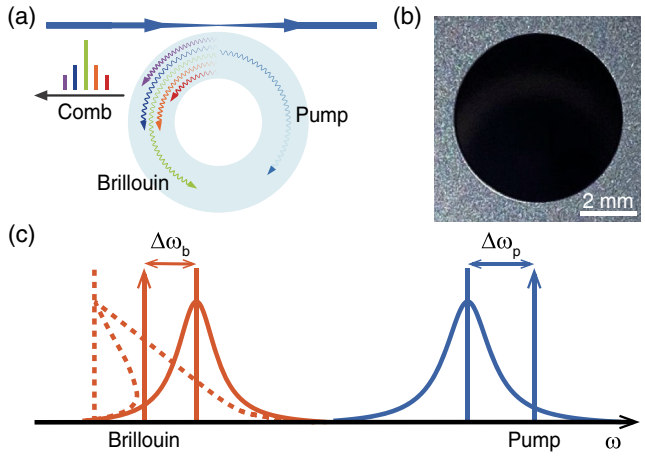

FIG. 1. (a) Schematic diagram of Brillouin-Kerr soliton frequency comb. (b) Photograph of the 6.3-mm-diameter disk resonator. (c) Illustration of red-detuned Brillouin laser with Kerr self-phase modulation. Dash orange curve, cavity response of Brillouin mode with Kerr self-phase modulation. See more details in Fig. S1 of the Supplemental Material [38].

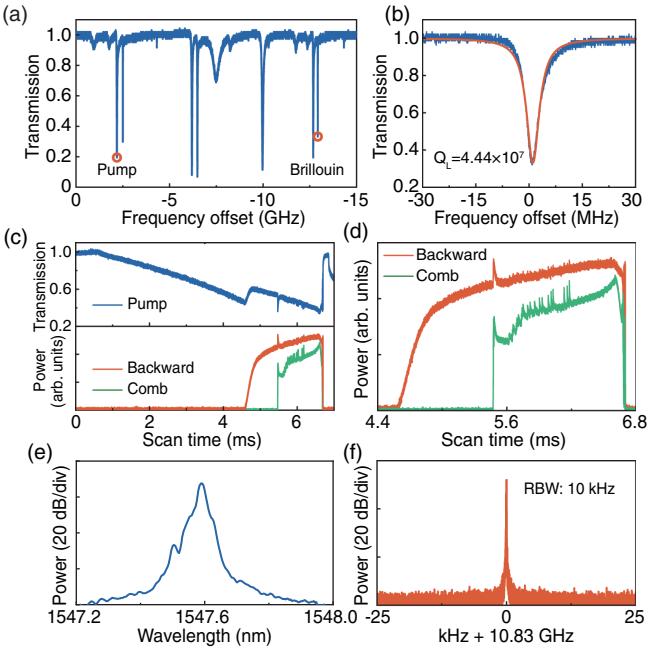

FIG. 2. (a) Typical transmission spectrum of the microresonator. (b) The transmission spectrum of the Brillouin mode. (c) The transmission power spectra of the pump laser, comb, and the backward laser (including reflected pump laser, Brillouin laser, and comb) at a pump power of 167 mW. (d) Close-up of transmission power spectra of the comb and backward laser, respectively. (e) The optical spectrum of backward laser before the comb generation. (f) The radiofrequency (rf) spectrum of the beat note between the reflected pump laser and Brillouin laser with a 10 kHz resolution bandwidth (RBW).

microwave signal based on the generated Brillouin-Kerr soliton microcomb.

In the experiment, a 6.3-mm-diameter silica microdisk resonator [Fig. 1(b)] with a thickness of 8 μm was fabricated using the previously established method [43]. The measured loaded Q factors for the Brillouin mode and the pump mode are 4.44×10^7 [Fig. 2(b)] and 8.42×10^6, respectively, and their corresponding intrinsic Q factors are 5.63×10^7 and 3.07×10^7. As shown in Fig. 2(a), the measured free spectral range of the Brillouin mode is 10.43 GHz, and the mode spacing between the pump mode and the Brillouin mode used for the Brillouin-Kerr soliton microcomb generation is 10.70 GHz.

In order to generate the Brillouin-Kerr frequency comb, the Brillouin mode and its corresponding mode family should exhibit anomalous group velocity dispersion while the pump mode and its corresponding mode family do not need to satisfy this requirement. Also, for the formation of a bright soliton, the generated Brillouin laser should be red detuned relative to the cavity mode [17,44], which can be ensured by the Kerr self-phase modulation effect of the Brillouin laser with a certain mode space between the pump and the Brillouin modes (see Supplemental Material [38], Sec. II). In the experiment, we first set the input pump laser to a relatively high power and scan the laser frequency with a speed of 243 MHz/ms. During the pump frequency tuning, the Brillouin lasing will occur first with a far blue-detuned input pump [Figs. 2(c) and 2(d)]. Figures 2(e) and 2(f) show, respectively, the measured optical spectrum of the Brillouin laser and rf spectrum of the beat note between the backscattered pump laser and the generated Brillouin laser before the formation of the Brillouin-Kerr comb. Note that the beat note here is different from the mode spacing [Fig. 2(a)] between the pump mode and Brillouin mode measured with a low optical power, since the pump and Brillouin modes, belonging to different transverse mode families, experience different redshifts under higher input pump power. As shown in Figs. 2(c) and 2(d), by gradually decreasing the frequency of the input pump, we can observe distinct soliton steps of the Brillouin-Kerr comb when the input pump laser is blue detuned, which indicates that the generated Brillouin laser is red detuned with respect to the Brillouin cavity mode [17]. Since the frequency of the generated Brillouin laser is insensitive to the fluctuation of input pump laser frequency [45] [also see Eq. (1) and Fig. S2(b) in Supplemental Material [38]], the experimentally obtained soliton steps are significantly broadened to dozens of MHz, which is much wider than that achieved in the previous work [20] with a silica microdisk resonator. The observation of the soliton steps with a blue-detuned input pump (although the Brillouin laser is red detuned) implies that the generated Kerr solitons can be thermally self-stable [37] even with the red-detuned Brillouin laser excitation (see Supplemental Material [38], Secs. IV and V). It is interesting to note that the observed soliton steps exhibit a "step-up" (the number of the solitons gradually increases with increasing pump wavelength) phenomenon, which is different from the previously

observed Kerr solitons [17]. This "step-up" phenomenon is attributed to the special line shape of the intracavity Brillouin laser power with the input pump frequency detuning that is induced by the interaction between the input pump and the generated Brillouin laser [45,46] (also see Supplemental Material [38], Sec. II). As a result, the intracavity Brillouin laser power will increase when increasing the pump wavelength. According to our numerical simulation, this interaction also extends the thermal self-stability of the pump into the red-detuning region (see Supplemental Material [38], Sec. IV).

To see how the generated Brillouin laser is red detuned and the soliton steps are broadened, we consider the phase-matching condition of the SBS process in a Kerr nonlinear cavity and obtain the frequency detuning of the Brillouin laser (see Supplemental Material [38], Sec. II for details):

$$\Delta\omega_{b,0} = \omega_{b,0} - \omega_{-,0} = \Delta\omega'_{b,0} + \Delta\omega''_{b,0}, \qquad (1)$$

where $\Delta\omega'_{b,0} = -[\gamma_m/(\gamma_m+\gamma_-)]g_2|a_{-,0}|^2$ and $\Delta\omega''_{b,0} = [\gamma_-/(\gamma_m+\gamma_-)](\Delta\omega_0+\Delta\omega_p)$. Here, $\Delta\omega_0=\omega_+-\omega_{-,0}-\Omega_0$ is the resonant frequency mismatch among the three modes: ω_+ (pump), $\omega_{-,0}$ (Brillouin), and Ω_0 (acoustic), and $\Delta\omega_p = \omega_p - \omega_+$ represents pump laser detuning. ω_p and $\omega_{b,0}$ are the pump and Brillouin laser frequencies, respectively. γ_m and γ_- represent the decay rates of the acoustic and Brillouin modes, respectively. g_2 is the Kerr nonlinear coupling coefficient and $a_{-,0}$ is the amplitude of the Brillouin laser. As shown in Eq. (1), the frequency shift of the Brillouin laser originates from two contributions, $\Delta\omega'_{b,0}$ and $\Delta\omega''_{b,0}$ [Fig. 1(c)], which are, respectively, determined by the Kerr self-phase modulation and the SBS processes. According to a previous study [17,44], the generation of the bright Kerr solitons requires a red-detuned pump. In the case of our Brillouin-Kerr solitons, this requirement implies $|\Delta\omega'_{b,0}| > \Delta\omega''_{b,0}$. On one hand, in the limit of $\gamma_m \gg \gamma_-$, we find $\Delta\omega'_{b,0} \approx -g_2|a_{-,0}|^2$ and $\Delta\omega''_{b,0} \approx (\gamma_-/\gamma_m)(\Delta\omega_0+\Delta\omega_p)$. As a result, for $\Delta\omega'_{b,0}$, we expect the redshift of the resonant Brillouin mode due to the self-phase modulation would give rise to an equivalent redshift on the Brillouin laser [Fig. 1(c)]. In this way, it makes a red-detuned Brillouin laser feasible easily in the cavity. On the other hand, $\Delta\omega''_{b,0}$ is determined by the frequency mismatch among the three modes plus the pump frequency detuning weighted by a small factor $\gamma_-/\gamma_m \ll 1$. This suggests that the large pump detuning modulation merely gives a small frequency shift for the Brillouin laser, because of the relatively small variation of $|a_{-,0}|^2$. With these, we conclude that this property is crucial for broadening the soliton steps when scanning the frequency of the input pump.

Owing to the wide soliton steps of the Brillouin-Kerr soliton microcomb, we can gradually access to the soliton states by manually adjusting the piezo of the input laser. In the measurements, by gradually tuning the frequency of the input pump laser into the soliton steps, multisoliton states can then be generated subsequently. After that, we use the backward-tuning method [47] to reduce the number of solitons until the single soliton is observed. As shown in Fig. 3(a), the blue curves represent the measured optical spectra of different soliton states with a repetition rate of 10.43 GHz. The orange curves show the fittings for the corresponding soliton states using the method described in Ref. [48]. The orange curve in III of Fig. 3(a) gives the single-soliton envelope of sech^2 fitting for a soliton pulse width of approximately 170 fs. The deviations between the fitting curves and the measured optical spectra at the blue side are due to the avoided mode crossing-induced dispersive wave [49,50] that is consistent with the measured dispersion [Fig. 3(c)]. Figures 4(a) and 4(b) show the measured optical spectrum of the generated soliton with a high resolution and spectrum of the forward propagating signal, respectively, which indicates that the cascaded Brillouin laser is not generated and the optical parametric oscillation process only occurs in the mode family of the Brillouin mode. To further confirm the single soliton state of the Brillouin-Kerr microcomb, we also performed autocorrelation measurement of the generated pulses. Figure 3(d) shows the measured autocorrelation trace with a pulse width of 231 fs, which is close to the result indicated from the optical spectrum. Also, the measured linewidth of the generated microwave signal [Fig. 3(b)] is as narrow as

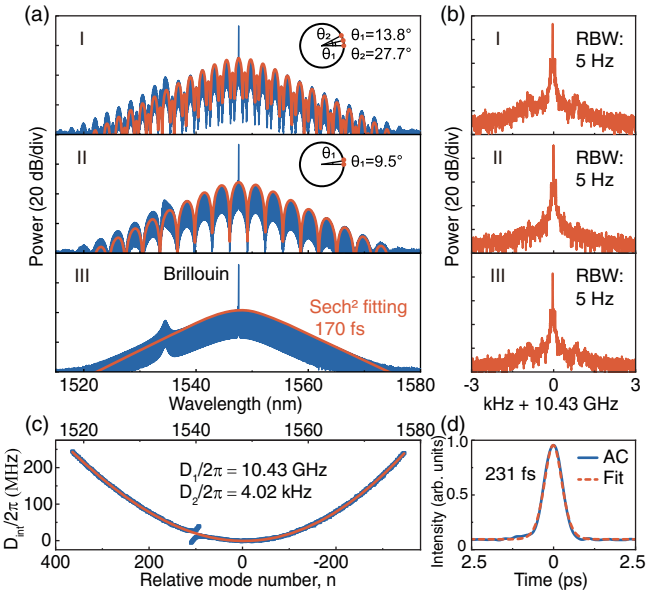

FIG. 3. (a) The optical spectra of different soliton states. I, II, and III show the measured optical spectra and fitted envelopes of the three-soliton state, two-soliton state, and single-soliton state, respectively. Insets show the relative positions of solitons circulating in the microdisk. (b) The rf spectra of the corresponding soliton repetition frequency in (a). (c) Measured dispersion $D_{\rm int}$ for the mode family of Brillouin mode. (d) Autocorrelation trace (AC trace) and autocorrelation function of sech^2 fitting for the single-soliton state in (a).

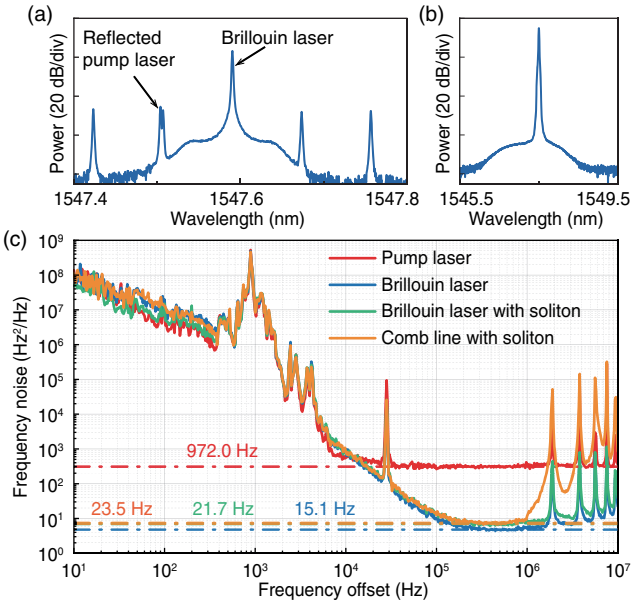

FIG. 4. (a) Close-up spectrum for the single-soliton state in Fig. 3(a) with 2 pm resolution nearby the Brillouin laser. (b) Forward optical spectrum for the single-soliton state in Fig. 3(a). (c) Single-sided frequency noise spectra of the pump laser, the Brillouin laser below parametric oscillation threshold, as well as the Brillouin laser and a comb line (1551.69 nm) with a single-soliton state. The dash-dotted lines represent the white-frequency-noise levels. The corresponding fundamental linewidths are also indicated.

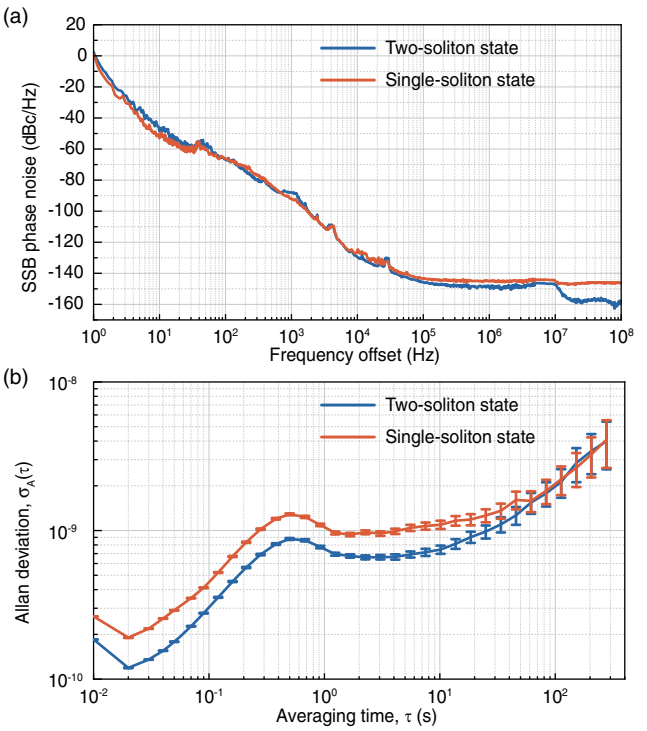

FIG. 5. (a) Single sideband (SSB) phase noise of the soliton repetition rate. (b) Allan deviation of the soliton repetition rate measured with 0.01 s gate time.

6 Hz which is much narrower than the previously reported results [17,20]. To explain the generation of the Brillouin-Kerr soliton microcomb, we have developed a theoretical model (see Supplemental Material [38], Secs. I and V) by fully taking into account the nonlinear four-wave mixing and SBS processes, as well as the interaction between them, which matches well with our experimental results. To characterize the linewidths of the Brillouin-Kerr comb lines, we carried out frequency noise measurements for the pump laser, the Brillouin laser below parametric oscillation threshold, as well as the Brillouin laser and a comb line (1551.69 nm) with a single-soliton state by using the correlated delayed self-heterodyne method [51]. As shown in Fig. 4(c), the fundamental linewidths determined from the white noise are 21.7 Hz for the Brillouin laser and 23.5 Hz for the measured comb line with a single-soliton state, respectively, which are much narrower than the fundamental linewidth of the pump laser. This result indicates that the linewidths of the comb lines are dependent on the generated Brillouin laser rather than on the pump laser [52], since here the intracavity Brillouin laser is used for the microcomb generation while the pump laser is used only for the Brillouin laser generation. Also, a small difference of the measured Brillouin laser linewidths can be found before and after the comb generation, which may result from the different pump detunings in these two processes [53].

Because of the narrow linewidths of the comb lines and the thermal stability of the Brillouin-Kerr soliton, the demonstrated microcomb allows us to produce a low-noise microwave signal with a free-running pump laser. In the previous works, both the Brillouin laser [32] and Kerr soliton microcombs [4–6,54] have been demonstrated for the generation of low-noise microwave signal. Those works typically employed active lock approaches, such as injection locking [5,6,54], Pound-Drever-Hall locking [5,6,54], and phase-lock loop [32], which require relatively complex optical and electrical components. In contrast, here by combining the advantages of both the Brillouin laser and the soliton microcomb generated in the same high-Q cavity, we realize a low-noise microwave signal generation using only a free-running pump laser. As one noticeable advantage, this setup makes the chip-integration of the system easy for practical microwave photonics applications. In the experiment, to measure the phase noise of the soliton's repetition rate, we filtered out the reflected pump laser and the Brillouin laser with two fiber Bragg grating filters and an optical fiber isolator, and then photomixed the frequency comb with a fast photodiode (see Supplemental Material [38], Fig. S5). Figure 5(a) shows the measured phase noise of the repetition rate of the Brillouin-Kerr solitons in the regions of single-soliton and two-soliton states, respectively, with optimized pump detunings. The obtained phase noise for the two-soliton state is −49 dBc/Hz at 10 Hz, −67 dBc/Hz at 100 Hz, −88 dBc/Hz at 1 kHz,

−130 dBc/Hz at 10 kHz, −146 dBc/Hz at 100 kHz, and −158 dBc/Hz at 20 MHz. Although the phase noise at low frequency offset is limited by the free-running pump laser, the achieved phase noise at high frequency offset (10 kHz–5 MHz) is even better or comparable to the result obtained in crystal resonator with self-injection locking [4]. Also, to the best of our knowledge, this achieved phase noise is already lower than that achieved in silica microdisk resonator using a single-mode dispersive wave at a 22 GHz carrier frequency [55]. The frequency stability of the repetition rate is characterized by the Allan deviation, as shown in Fig. 5(b). The measured frequency stability for the two-soliton state is 7.5×10^{-10} at 1 s and 2.1×10^{-9} at 100 s average time, respectively. We attribute this high stability of the repetition rate to the insensitivity of the generated intracavity Brillouin laser to the frequency fluctuation of pump laser [see Eq. (1) and Refs. [29,45,56]] and the thermal self-stability of the Brillouin-Kerr soliton. Note that the bump at 0.5 s average time in Fig. 5(b) may be caused by the mechanical vibrations of the measurement system, which can be avoided by photonic packaging technique [5].

In conclusion, we have experimentally and theoretically demonstrated a Brillouin-Kerr soliton microcomb with narrow-linewidth comb lines and stable repetition rate. In contrast to the previous work with a red-detuned pump, our approach with blue-detuned pump makes the system be thermally self-stabilized. We have also obtained the ultralow-noise microwave signal based on this soliton microcomb with only a free-running pump laser. For practical applications, to ensure the generation of the Brillouin-Kerr solitons with a fixed repetition rate, the mode space between the pump and Brillouin modes can be engineered by controlling the thickness and wedge angle of the microdisk resonator while keeping the diameter of the microcavity fixed. Our scheme should also be applicable to other material platforms such as crystal and silicon nitride resonators [30,57], where both Kerr soliton and Brillouin nonlinearity have already been separately demonstrated. In particular, our approach can be adapted in the midinfrared wavelength range where the narrow-linewidth pump laser is limited. Moreover, turn-key operation [58] for such thermally self-stabilized Kerr soliton microcomb from the current scheme will be beneficial for future applications.

We thank Professor Kerry Vahala for helpful comments and suggestions on this work. We also thank Junqiu Liu, Yuhang Li, Qi-fan Yang, and Fei Xu for helpful discussions. This research was supported by the National Key R&D Program of China (2017YFA0303703, 2016YFA0302500), the National Natural Science Foundation of China (NSFC) (61922040, 11621091), Guangdong Major Project of Basic and Applied Basic Research (2020B0301030009), and the Fundamental Research Funds for the Central Universities (021314380170).

*These authors contributed equally.
†jxs@nju.edu.cn

[1] T. J. Kippenberg, A. L. Gaeta, M. Lipson, and M. L. Gorodetsky, Dissipative Kerr solitons in optical microresonators, Science **361**, eaan8083 (2018).
[2] A. L. Gaeta, M. Lipson, and T. J. Kippenberg, Photonic-chip-based frequency combs, Nat. Photonics **13**, 158 (2019).
[3] P. Marin-Palomo, J. N. Kemal, M. Karpov, A. Kordts, J. Pfeifle, M. H. P. Pfeiffer, P. Trocha, S. Wolf, V. Brasch, M. H. Anderson *et al.*, Microresonator-based solitons for massively parallel coherent optical communications, Nature (London) **546**, 274 (2017).
[4] W. Liang, D. Eliyahu, V. S. Ilchenko, A. A. Savchenkov, A. B. Matsko, D. Seidel, and L. Maleki, High spectral purity Kerr frequency comb radio frequency photonic oscillator, Nat. Commun. **6**, 7957 (2015).
[5] J. Liu, E. Lucas, A. S. Raja, J. He, J. Riemensberger, R. N. Wang, M. Karpov, H. Guo, R. Bouchand, and T. J. Kippenberg, Photonic microwave generation in the *X*- and *K*-band using integrated soliton microcombs, Nat. Photonics **14**, 486 (2020).
[6] E. Lucas, P. Brochard, R. Bouchand, S. Schilt, T. Südmeyer, and T. J. Kippenberg, Ultralow-noise photonic microwave synthesis using a soliton microcomb-based transfer oscillator, Nat. Commun. **11**, 374 (2020).
[7] M.-G. Suh, Q.-F. Yang, K. Y. Yang, X. Yi, and K. J. Vahala, Microresonator soliton dual-comb spectroscopy, Science **354**, 600 (2016).
[8] A. Dutt, C. Joshi, X. Ji, J. Cardenas, Y. Okawachi, K. Luke, A. L. Gaeta, and M. Lipson, On-chip dual-comb source for spectroscopy, Sci. Adv. **4**, e1701858 (2018).
[9] M.-G. Suh and K. J. Vahala, Soliton microcomb range measurement, Science **359**, 884 (2018).
[10] P. Trocha, M. Karpov, D. Ganin, M. H. P. Pfeiffer, A. Kordts, S. Wolf, J. Krockenberger, P. Marin-Palomo, C. Weimann, S. Randel *et al.*, Ultrafast optical ranging using microresonator soliton frequency combs, Science **359**, 887 (2018).
[11] M.-G. Suh, X. Yi, Y.-H. Lai, S. Leifer, I. S. Grudinin, G. Vasisht, E. C. Martin, M. P. Fitzgerald, G. Doppmann, J. Wang *et al.*, Searching for exoplanets using a microresonator astrocomb, Nat. Photonics **13**, 25 (2019).
[12] E. Obrzud, M. Rainer, A. Harutyunyan, M. H. Anderson, M. Geiselmann, B. Chazelas, S. Kundermann, S. Lecomte, M. Cecconi, A. Ghedina *et al.*, A microphotonic astrocomb, Nat. Photonics **13**, 31 (2019).
[13] P. J. Marchand, J. C. Skehan, J. Riemensberger, J.-J. Ho, M. H. P. Pfeiffer, J. Liu, C. Hauger, T. Lasser, and T. J. Kippenberg, Soliton microcomb based spectral domain optical coherence tomography, arXiv:1902.06985.
[14] D. T. Spencer, T. Drake, T. C. Briles, J. Stone, L. C. Sinclair, C. Fredrick, Q. Li, D. Westly, B. R. Ilic, A. Bluestone *et al.*, An optical-frequency synthesizer using integrated photonics, Nature (London) **557**, 81 (2018).
[15] Z. L. Newman, V. Maurice, T. Drake, J. R. Stone, T. C. Briles, D. T. Spencer, C. Fredrick, Q. Li, D. Westly, B. R. Ilic *et al.*, Architecture for the photonic integration of an optical atomic clock, Optica **6**, 680 (2019).

[16] A. Kovach, D. Chen, J. He, H. Choi, A. H. Dogan, M. Ghasemkhani, H. Taheri, and A. M. Armani, Emerging material systems for integrated optical Kerr frequency combs, Adv. Opt. Photonics **12**, 135 (2020).
[17] T. Herr, V. Brasch, J. D. Jost, C. Y. Wang, N. M. Kondratiev, M. L. Gorodetsky, and T. J. Kippenberg, Temporal solitons in optical microresonators, Nat. Photonics **8**, 145 (2014).
[18] J. Liu, G. Huang, R. N. Wang, J. He, A. S. Raja, T. Liu, N. J. Engelsen, and T. J. Kippenberg, High-yield wafer-scale fabrication of ultralow-loss, dispersion-engineered silicon nitride photonic circuits, arXiv:2005.13949.
[19] J. Liu, A. S. Raja, M. Karpov, B. Ghadiani, M. H. P. Pfeiffer, B. Du, N. J. Engelsen, H. Guo, M. Zervas, and T. J. Kippenberg, Ultralow-power chip-based soliton microcombs for photonic integration, Optica **5**, 1347 (2018).
[20] X. Yi, Q.-F. Yang, K. Y. Yang, M.-G. Suh, and K. Vahala, Soliton frequency comb at microwave rates in a high-Q silica microresonator, Optica **2**, 1078 (2015).
[21] V. Brasch, M. Geiselmann, M. H. P. Pfeiffer, and T. J. Kippenberg, Bringing short-lived dissipative Kerr soliton states in microresonators into a steady state, Opt. Express **24**, 29312 (2016).
[22] C. Joshi, J. K. Jang, K. Luke, X. Ji, S. A. Miller, A. Klenner, Y. Okawachi, M. Lipson, and A. L. Gaeta, Thermally controlled comb generation and soliton modelocking in microresonators, Opt. Lett. **41**, 2565 (2016).
[23] E. Obrzud, S. Lecomte, and T. Herr, Temporal solitons in microresonators driven by optical pulses, Nat. Photonics **11**, 600 (2017).
[24] J. R. Stone, T. Briles, T. E. Drake, D. T. Spencer, D. R. Carlson, S. A. Diddams, and S. B. Papp, Thermal and Nonlinear Dissipative-Soliton Dynamics in Kerr-Microresonator Frequency Combs, Phys. Rev. Lett. **121**, 063902 (2018).
[25] Z. Lu, W. Wang, W. Zhang, S. T. Chu, B. E. Little, M. Liu, L. Wang, C.-L. Zou, C.-H. Dong, B. Zhao *et al.*, Deterministic generation and switching of dissipative Kerr soliton in a thermally controlled micro-resonator, AIP Adv. **9**, 025314 (2019).
[26] S. Zhang, J. M. Silver, L. D. Bino, F. Copie, M. T. M. Woodley, G. N. Ghalanos, A. Ø. Svela, N. Moroney, and P. Del'Haye, Sub-milliwatt-level microresonator solitons with extended access range using an auxiliary laser, Optica **6**, 206 (2019).
[27] H. Zhou, Y. Geng, W. Cui, S.-W. Huang, Q. Zhou, K. Qiu, and C. W. Wong, Soliton bursts and deterministic dissipative Kerr soliton generation in auxiliary-assisted microcavities, Light Sci. Appl. **8**, 50 (2019).
[28] B. J. Eggleton, C. G. Poulton, P. T. Rakich, M. J. Steel, and G. Bahl, Brillouin integrated photonics, Nat. Photonics **13**, 664 (2019).
[29] J. Li, H. Lee, T. Chen, and K. J. Vahala, Characterization of a high coherence, Brillouin microcavity laser on silicon, Opt. Express **20**, 20170 (2012).
[30] S. Gundavarapu, G. M. Brodnik, M. Puckett, T. Huffman, D. Bose, R. Behunin, J. Wu, T. Qiu, C. Pinho, N. Chauhan *et al.*, Sub-hertz fundamental linewidth photonic integrated Brillouin laser, Nat. Photonics **13**, 60 (2019).
[31] J. Li, M.-J. Suh, and K. Vahala, Microresonator Brillouin gyroscope, Optica **4**, 346 (2017).
[32] J. Li, H. Lee, and K. Vahala, Microwave synthesizer using an on-chip Brillouin oscillator, Nat. Commun. **4**, 2097 (2013).
[33] D. Braje, L. Hollberg, and S. Diddams, Brillouin-Enhanced Hyperparametric Generation of an Optical Frequency Comb in a Monolithic Highly Nonlinear Fiber Cavity Pumped by a cw Laser, Phys. Rev. Lett. **102**, 193902 (2009).
[34] M. Asano, Y. Takeuchi, S. K. Ozdemir, R. Ikuta, L. Yang, N. Imoto, and T. Yamamoto, Stimulated Brillouin scattering and Brillouin-coupled four-wave-mixing in a silica microbottle resonator, Opt. Express **24**, 12082 (2016).
[35] D. Farnesi, G. Righini, G. N. Conti, and S. Soria, Efficient frequency generation in phoXonic cavities based on hollow whispering gallery mode resonators, Sci. Rep. **7**, 44198 (2017).
[36] Y. Huang, Q. Li, J. Han, Z. Jia, Y. Yu, Y. Yang, J. Xiao, J. Wu, D. Zhang, Y. Huang *et al.*, Temporal soliton and optical frequency comb generation in a Brillouin laser cavity, Optica **6**, 1491 (2019).
[37] T. Carmon, L. Yang, and K. J. Vahala, Dynamical thermal behavior and thermal self-stability of microcavities, Opt. Express **12**, 4742 (2004).
[38] See Supplemental Material at http://link.aps.org/supplemental/10.1103/PhysRevLett.126.063901 for details of the theoretical models, numerical simulations, and experimental methods, which includes Refs. [39–42].
[39] Y. K. Chembo and N. Yu, Modal expansion approach to optical-frequency-comb generation with monolithic whispering-gallery-mode resonators, Phys. Rev. A **82**, 033801 (2010).
[40] Q.-F. Yang, X. Yi, K. Y. Yang, and K. Vahala, Stokes solitons in optical microcavities, Nat. Phys. **13**, 53 (2017).
[41] R. W. Boyd, *Nonlinear Optics*, 3rd ed. (Academic Press, New York, 2007).
[42] T. Hansson, D. Modotto, and S. Wabnitz, On the numerical simulation of Kerr frequency combs using coupled mode equations, Opt. Commun. **312**, 134 (2014).
[43] H. Lee, T. Chen, J. Li, K. Y. Yang, S. Jeon, O. Painter, and K. J. Vahala, Chemically etched ultrahigh-Q wedge-resonator on a silicon chip, Nat. Photonics **6**, 369 (2012).
[44] C. Godey, I. V. Balakireva, A. Coillet, and Y. K. Chembo, Stability analysis of the spatiotemporal Lugiato-Lefever model for Kerr optical frequency combs in the anomalous and normal dispersion regimes, Phys. Rev. A **89**, 063814 (2014).
[45] L. William, S. B. Papp, and S. A. Diddams, Noise and dynamics of stimulated-Brillouin-scattering microresonator lasers, Phys. Rev. A **91**, 053843 (2015).
[46] D. A. Korobko, I. O. Zolotovskii, V. V. Svetukhin, A. V. Zhukov, A. N. Fomin, C. V. Borisova, and A. A. Fotiadi, Detuning effects in Brillouin ring microresonator laser, Opt. Express **28**, 4962 (2020).
[47] H. Guo, M. Karpov, E. Lucas, A. Kordts, M. H. P. Pfeiffer, V. Brasch, G. Lichachev, V. E. Lobanov, M. L. Gorodetsky, and T. J. Kippenberg, Universal dynamics and deterministic switching of dissipative Kerr solitons in optical microresonators, Nat. Phys. **13**, 94 (2017).
[48] V. Brasch, M. Geiselmann, T. Herr, G. Lihachev, M. H. P. Pfeiffer, M. L. Gorodetsky, and T. J. Kippenberg, Photonic

chip-based optical frequency comb using soliton Cherenkov radiation, Science **351**, 357 (2016).
[49] Q.-F. Yang, X. Yi, K. Y. Yang, and K. Vahala, Spatial-mode-interaction-induced dispersive waves and their active tuning in microresonators, Optica **3**, 1132 (2016).
[50] A. B. Matsko, W. Liang, A. A. Savchenkov, D. Eliyahu, and L. Maleki, Optical Cherenkov radiation in overmoded microresonators, Opt. Lett. **41**, 2907 (2016).
[51] S. Camatel and V. Ferrero, Narrow linewidth CW laser phase noise characterization methods for coherent transmission system applications, J. Lightwave Technol. **26**, 3048 (2008).
[52] P. Liao, C. Bao, A. Kordts, M. Karpov, M. H. P. Pfeiffer, L. Zhang, A. Mohajerin-Ariaei, Y. Cao, A. Almaiman, M. Ziyadi *et al.*, Dependence of a microresonator Kerr frequency comb on the pump linewidth, Opt. Lett. **42**, 779 (2017).
[53] Z. Yuan, H. Wang, L. Wu, M. Gao, and K. Vahala, Linewidth enhancement factor in a microcavity Brillouin laser, Optica **7**, 1150 (2020).
[54] W. Weng, E. Lucas, G. Lihachev, V. E. Lobanov, H. Guo, M. L. Gorodetsky, and T. J. Kippenberg, Spectral Purification of Microwave Signals with Disciplined Dissipative Kerr Solitons, Phys. Rev. Lett. **122**, 013902 (2019).
[55] X. Yi, Q.-F. Yang, X. Zhang, K. Y. Yang, X. Li, and K. Vahala, Single-mode dispersive waves and soliton microcomb dynamics, Nat. Commun. **8**, 14869 (2017).
[56] I. S. Grudinin, A. B. Matsko, and L. Maleki, Brillouin Lasing with a CaF_2 Whispering Gallery Mode Resonator, Phys. Rev. Lett. **102**, 043902 (2009).
[57] F. Gyger, J. Liu, F. Yang, J. He, A. S. Raja, R. N. Wang, S. A. Bhave, T. J. Kippenberg, and L. Thévenaz, Observation of Stimulated Brillouin Scattering in Silicon Nitride Integrated Waveguides, Phys. Rev. Lett. **124**, 013902 (2020).
[58] B. Shen, L. Chang, J. Liu, H. Wang, Q.-F. Yang, C. Xiang, R. N. Wang, J. He, T. Liu, W. Xie *et al.*, Integrated turnkey soliton microcombs, Nature (London) **582**, 365 (2020).